Cathode Property of Na_2C_xO_x [x = 4, 5, and 6] and K_2C_6O_6 for Sodium-ion Batteries

Chihara, Kuniko
Interdisciplinary Graduate School of Engineering Sciences, Kyushu University

Ito, Masato
Institute for Materials Chemistry and Engineering, Kyushu University

Kitajou, Ayuko
Institute for Materials Chemistry and Engineering, Kyushu University

Okada, Shigeto
Institute for Materials Chemistry and Engineering, Kyushu University

https://doi.org/10.5109/1808304

出版情報：Evergreen. 4 (1), pp.1-5, 2017-03. Green Asia Education Center
バージョン：

Cathode Property of $Na_2C_xO_x$ [x = 4, 5, and 6] and $K_2C_6O_6$ for Sodium-ion Batteries

Kuniko Chihara[1], Masato Ito[2], Ayuko Kitajou[2], Shigeto Okada[2,*]

[1] Interdisciplinary Graduate School of Engineering Sciences, Kyushu University, Japan

[2] Institute for Materials Chemistry and Engineering, Kyushu University, Japan

*Corresponding author, E-mail: s-okada@cm.kyushu-u.ac.jp

(Received November 17, 2016; accepted December 6, 2016).

Sodium-ion batteries now become a strong alternative candidate for lithium-ion batteries due to abundant Na resources, and organic electrode active materials for sodium-ion batteries also have possibility to bring additional cost reduction. Although many organic-based active materials have been researched as cathode materials for lithium-ion batteries, few works have been conducted for sodium-ion batteries. In this study, the cathode properties of several organic compounds of sodium rhodizonate analogs, $Na_2C_xO_x$ [x = 4 and 5] and $K_2C_6O_6$ were newly investigated. Among them, it was revealed that $Na_2C_5O_5$ and $Na_2C_6O_6$ deliver large first discharge capacity close to 200 mAh g^{-1} and exhibit reversible sodium insertion/de-insertion of 1.35 and 1.25Na, respectively, with good cycle performance.

Keywords: sodium-ion battery, organic material, sodium oxocarbon salt

1. Introduction

Lithium-ion batteries (LIBs) have been widely used due to the high energy density and good cyclability as power storage for portable electronic devices and electric vehicles. However, commonly used cathodes for LIBs such as $LiCoO_2$ are synthesized from limited mineral resources, and thus inexpensive minor-metal free materials, which can be derived from more abundant resources, have become increasingly desirable along with the world's growing demand on power storage. As a strategy to solve this ecological concern, researchers have devoted themselves to find new battery technology with using alternative materials. The layered rocksalt-type $NaMO_2$ (M : 3d series transition metal) cathodes for Na secondary batteries were reported as early as in 1980's[1,2], while it is only recently that minor-metal free sodium ion batteries (SIBs) with sodium-based active materials and electrolytes gain renewed attention in view of abundant resources. The reported cathode active materials with relatively large capacity for SIBs are limited to some special material groups, and their common features are an open structure with two-dimensional layered or three-dimensional corner sharing matrix[3-8] except alluaudite-type $Na_2Fe_2(SO_4)_3$[9]. We, therefore, expect organic materials could also become strong candidates for SIBs due to their low density and stacking structure. Especially, organic compounds with lamellar stacking structure would be capable of accepting repeated insertion and extraction of the large sodium ion, and they are promising materials to be useful countermeasures in the energy crisis. Researches of organic active materials can be traced back to the discovery of conductive polymers in 1970's, and Heeger et al. have proposed an application of $(CH)_x$ conducting organic polymer as the electrode active material of light weight rechargeable batteries[10]. So far, many organic active materials for LIBs have been reported, including organic sulfide polymers[11-14] and organic radical cathode[15-18]. Very recently, several organic-based cathodes for SIBs have been proposed[19,20]. We also reported the electrochemical propertied of disodium rhodizonate, $Na_2C_6O_6$, and demonstrated its rechargeable discharge/ charge cycle in a full cell configuration with Na predoped hard carbon[21]. Disodium rhodizonate shows multi-electron reaction and surprisingly high sodium ion kinetics in charge and discharge processes. In this work, we investigate $Na_2C_5O_5$, $Na_2C_4O_4$, and $K_2C_6O_6$ as series of $Na_2C_6O_6$ to evaluate their potential as new cathode active materials and compare their cathode performance.

2. Experimental

$H_2C_4O_4$ and $H_2C_5O_5$ were purchased from Tokyo chemical industry Co., Ltd. $Na_2C_4O_4$ and $Na_2C_5O_5$ were synthesized by following substitution reaction; $H_2C_xO_x$ + 2NaOH -> $Na_2C_xO_x$ + H_2O [x = 4 and 5] as described in the reported patent[22]. $Na_2C_6O_6$ (Marek KGaA) and $K_2C_6O_6$ (Wako pure chemical industries, Ltd.) were purchased and used without further purification. The prepared or purchased $Na_2C_XO_X$ [x = 4, 5, and 6] and

$K_2C_6O_6$ powders were first dry-ball-milled with acetylene black (AB) (DENKA Co., Ltd.) under an Ar atmosphere with the weight ratio of oxocarbon salt : AB = 70 : 25. The resulting composite powders were mixed with 5 wt% polytetrafluoroethylene (PTFE) binder to fabricate pellet electrodes with a diameter of 10 mm. The obtained pellets were then dried under ca. 110 ˚C overnight before assembling cells. The electrode was electrochemically sodiated and disodiated with a non-aqueous electrolyte of 1M $NaPF_6$/PC (Kisida Chemical Co., Ltd.) or 1M $NaClO_4$/PC (Tomiyama Pure Chemicals Industries, Ltd.) and a polypropylene separator (model 3501; Celgard, LLC.) against Na metal (Sigma-Aldrich Co. LLC.) in a 2032 coin-type cell. Electrochemical measurements for the cells were carried out in galvanostatic mode under the constant current of 0.2 mA cm^{-2}. In order to prepare samples for structural analysis after sodiation and desodiation, the electrochemical measurement was stopped at each preset voltage, and the charged or discharged electrodes were carefully taken out from the cells after being left for 24 h in the cells to reach equilibrium state. After aging, the electrodes were washed and soaked in dimethyl carbonate (DMC, Tomiyama Pure Chemicals Industries, Ltd.). They were then dried in the Ar-filled grove- box under vacuum.

The *ex-situ* X-ray powder diffraction (XRD) measurements were performed for the various charged and discharged states using Cu-Kα radiation (50 kV and 300 mA, Cu-Kα, RINT2100HR/PC, RIGAKU Corp.) from 2 θ = 10 - 80° with 0.02° step scan at a rate of 0.15° min^{-1}. All of the *ex-situ* XRD patterns were taken under Ar using an air-tight specimen holder (Bruker Corp.) in order to avoid oxidation and hydration by air.

3. Results and Discussion

3.1 Electrochemical properties of $Na_2C_xO_x$

Figure 1 (a - c) show the discharge and charge profiles of $Na_2C_xO_x$ [x = 4, 5, and 6] against Na metal in 1 M $NaClO_4$/PC. The cut off voltage ranges were optimized to 0.1 - 2.0, 1.0 - 2.0, and 1.5 - 2.9 V for $Na_2C_4O_4$, $Na_2C_5O_5$, and $Na_2C_6O_6$, respectively. $Na_2C_4O_4$ shows first discharge capacity of ca. 100 mAh g^{-1} with a small plateau at 0.6 V and $Na_2C_4O_4$ is not electrochemically active in following cycles (Fig.1(a)). In contrast, as showed in Fig.1 (b) and (c), $Na_2C_5O_5$ and $Na_2C_6O_6$ delivers large first discharge capacity of 207 mAh g^{-1} and 236 mAh g^{-1} corresponding to 1.44Na and 1.89Na insertion, respectively. Although $Na_2C_6O_6$ shows excellent reversibility as have already we reported in the previous report, [21] its irreversible capacity is relatively large to be 67.3 mAh g^{-1} corresponding to 0.53Na. On the other hand, $Na_2C_5O_5$ exhibits less irreversible capacity of 27.7 mAh g^{-1} (0.19Na), and shows the good cyclability as shown in Fig. 2 (a). The discharge capacity of $Na_2C_5O_5$ is lager in 1M $NaClO_4$/PC electrolyte than that in 1M $NaPF_6$/PC for first few cycles, however more stable cycle performance is obtained in 1M $NaPF_6$/PC. In the dQ/dV curves in Fig. 2 (b) and (c), large anodic peaks appear at 1.5 V for $Na_2C_5O_5$ and 1.97 V for $Na_2C_6O_6$, and several corresponding cathodic peaks are seen in the following charge process. After the first cycle, the reversible anodic/cathodic redox peaks are observed in the both cathodes and each polarization between the anodic/cathodic peaks was less than 0.2 V.

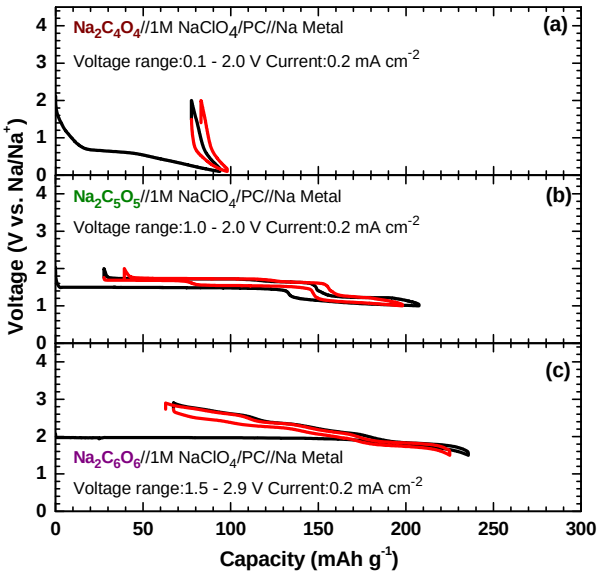

Fig. 1: Charge and discharge profiles of (a) $Na_2C_4O_4$, (b) $Na_2C_5O_5$, and (c) $Na_2C_6O_6$, respectively.

As stated above, $Na_2C_6O_6$ and $Na_2C_5O_5$ proved to be very attractive active materials in terms of energy efficiency. However, in consideration of practical usage, we have to solve a problem of the irreversible capacity in the first discharge, especially in $Na_2C_6O_6$. To improve the cathode performances, it was important to understand the reaction mechanism in organic cathodes during charge and discharge cycling.

Instead of the redox of transition metal in inorganic cathode, π-electrons on C-C or C-O multiple bonds should play major role to drive charge and discharge processes in organic cathodes. Formally, oxocarbon dianions have an extreme structure with one endocyclic C=C bond and different numbers of exocyclic C=O bonds depending on their ring size.[23] Therefore, the differences in electrochemical performances depending on the number of x in $Na_2C_xO_x$ were mainly attributable to the redox behavior of π-electrons over C=O bonds in a series of $Na_2C_xO_x$.

3.2 Electrochemical properties of $Na_2C_6O_6$ and $K_2C_6O_6$,

$K_2C_6O_6$ is historically significant as one of the oldest synthetic organic compounds[23] but it has received less attention as functional materials until recently[24]. Figure

3(a) and (b) show the electrochemical property of $Na_2C_6O_6$ and $K_2C_6O_6$ in 1M $NaClO_4$/PC electrolyte, respectively. The discharge cutoff voltage was set down to 1.0 V in both cases. The first discharge capacity of $Na_2C_6O_6$ increases to 312.8 mAh g^{-1}, which corresponds to 2.5Na insertion, and its reversible capacity reaches to

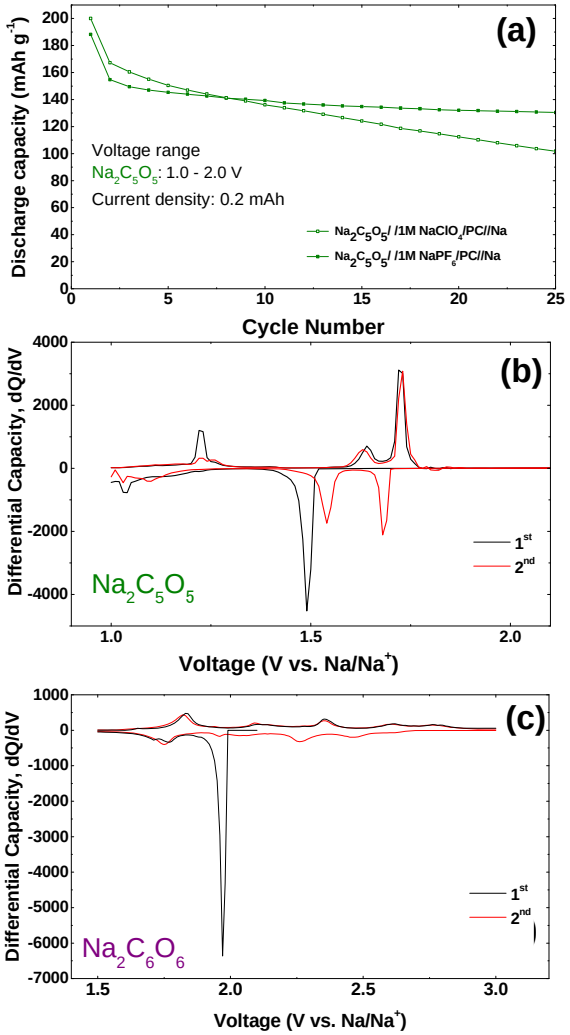

Fig. 2: (a) Cyclabilities of $Na_2C_5O_5$ and $Na_2C_6O_6$ in 1 M $NaClO_4$/PC and 1 M $NaPF_6$/PC electrolyte. dQ/dV curves of (b) $Na_2C_5O_5$ and (c) $Na_2C_6O_6$, respectively

more than 2.1Na reaction of 267 mAh g^{-1}. The discharge capacity reduces after few cycles, resulting in 190.6 mAh/g at 5th and 174.4 mAh/g at 10th cycles. $K_2C_6O_6$ also shows large reversible capacity over 200 mAh g^{-1} albeit slightly smaller than that for Na congener. It is also notable that the irreversible capacity for $K_2C_6O_6$ is markedly smaller than that for $Na_2C_6O_6$. Unfortunately, however, its discharge capacity gradually decreases on cycles, resulting in only 0.2 Na at 10th cycles. Interestingly, these two components are regarded as rhodizonic cation analogs, however their electrochemical properties including charge and discharge profiles, reacting Na amounts, and discharge degradation tendency are totally different. The difference between the charge and discharge profiles suggests that the cathode properties are delicately influenced by the cation in $A_2C_6O_6$ rhodizonate-type cathodes. Similar difference has been also observed even in inorganic materials such as $LiCoO_2$ and $NaCoO_2$[25].

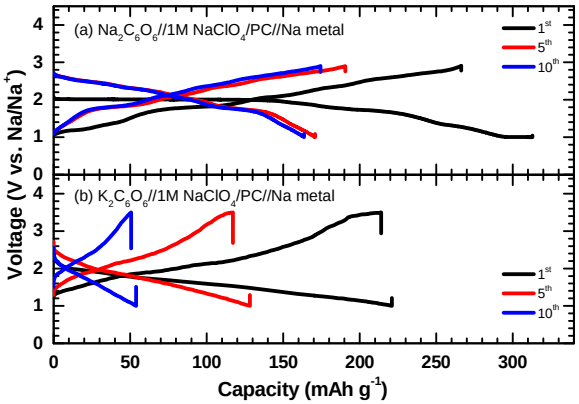

Fig. 3: Comparisons in charge and discharge profiles of (a) $Na_2C_6O_6$ and (b) $K_2C_6O_6$. $Na_2C_6O_6$ and $K_2C_6O_6$ were cycled in 1.0 - 2.9 V and 1.0 - 3.5 V, respectively. The current density were 0.2 mA cm^{-2} in both cases.

3.3 Structural change of $Na_2C_6O_6$ during charge and discharge process

Dinnebier *et al.* have revealed the layer structure of Disodium rhodizonate by Rietveld refinement of synchrotron radiated high resolution X-ray diffraction[26]. The layers of hexagonally packed Na^+ alternate with layers of similarly packed $C_6O_6^{2-}$, and Na^+ lies *a/4* above $C_6O_6^{2-}$. All sodium cations are surrounded by eight O atoms of four rhodizonate anions in the solid state. In order to gain an insight for phase change of $Na_2C_6O_6$ along with electrochemical sodiation and desodiation, *ex-situ* XRD measurements were performed on the first cycle. Figure 6 shows the XRD profile patterns for charged and discharged $Na_2C_6O_6$ electrodes. As for the pattern of $Na_2C_6O_6$ at 1Na/mol discharge (124 mAh/g), which is at the middle of plateau region at 2.0 V, a new phase was detected with a decrease of the original phase. The first-principle calculation[27] has proposed a new C_6O_6 stacking structure for $Na_xC_6O_6$ (x > 2), which is distinct from that for x = 2. The coexistence of the two different phases in Fig. 4 (b) is consistent with the flat discharge plateau at 2 V as shown in Fig. 1 (c). After discharge down to 1.8 V (Fig. 4(c)), the original disodium rhodizonate phase was completely disappeared and the flat discharge plateau was also lost (Fig. 1 (c)). In the following charge process, the *ex-situ* XRD pattern of the electrode charged up to 2.9 V showed peak shift behavior as in the solid state reaction and some of diffraction peaks reappeared at the original position (Fig. 4(e)).

However, after the second cycle, the discharge/ charge profile became the slope type and the two-phase coexistence was observed only in the 2.0 V plateau

region at the 1st discharge. We believe that the pattern change in our *ex-situ* XRD is responsible for two-phase reaction of $Na_2C_6O_6$, although further studies are necessary to describe precisely the three-dimensional structural difference of the two phases that should be highly associated with the change of the local molecular structure of $Na_2C_6O_6$ upon charge and discharge, which will be reported in elsewhere soon.

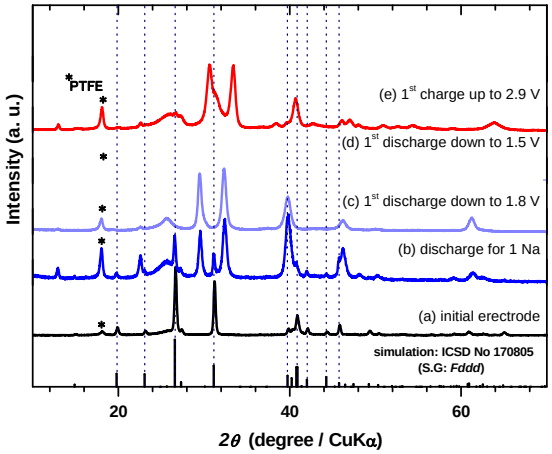

Fig. 4: *Ex-situ* XRD patterns of $Na_2C_6O_6$ at the state of (a) initial, discharge to (b) 1Na, (c) to 1.8 V, (d) to 1.5 V, and charge to (e) 2.9 V, respectively.

4. Conclusion

Electrochemical properties of oxocarbon salts including $Na_2C_xO_x$ [x = 4, 5, and 6] and $K_2C_6O_6$ have been examined as cathode active materials for SIBs. Among them, $Na_2C_5O_5$ and $Na_2C_6O_6$ showed marked cycle performances with small discharge/charge overpotential, which are suitable for their application to SIBs. *Ex-situ* XRD measurement for the samples during 1st charge and discharge was performed to gain an insight for the structural change of $Na_2C_6O_6$ in the sodium cell. Our results suggested that the original solid phase of $Na_2C_6O_6$ transforms into two new phases upon discharge down to 1.8 V, while the resulting phases disappear and reappear upon the subsequent charge and discharge.

Acknowledgements

This work was financially supported by the Elements Strategy Initiative for Catalysts and Batteries Project and the Cooperative Research Program of "Network Joint Research Center for Materials and Devices", MEXT, Japan.

References

1) J. J. Braconnier, C. Delmas, C. Fouassier, P. Hagenmuller, *Mater. Res. Bull.*, **15**, 1797 (1980).
2) S. Miyazaki, S. Kikkawa, M. Koizumi, *Synthetic Metals*, **6**, 211 (1983).
3) J. Li, H. Zhan, L. Zhou, S. Deng, Z. Li, Y. Zhou, *Electrochem. Commun.*, **6**, 515 (2004).
4) J. Zhao, L. -W. Zhao, N. Dimov, S. Okada, T. Nishida, *J. Electrochem. Soc.*, **160**, 5, A3077 (2013).
5) T. B. Kim, J. W. Choi, H. S. Ryu, G. B. Cho, K. W. Kim, J. H. Ahn, K. K. Cho, H. J. Ahn, *J. Power Sources*, **174**, 1275 (2007).
6) K. Chihara, A. Kitajou, I. D. Gocheva, S. Okada, J. Yamaki, *J. Power Sources*, **227**, 80 (2013).
7) B. L. Ellis, W. R. M. Makahnouk, Y. Makimura, K. Toghill, L. F. Nazar. *Nature Mater.*, **6**, 749 (2007).
8) P. Barpanda, T. Ye, S. Nishimura, S. C. Chung, Y. Yamada, M. Okubo, H. Zhou, A. Yamada, *Electrochem. Commun.*, **24**, 116 (2012).
9) P. Barpanda, G. Oyama, S. Nishimura, S. -C. Chung, A. Yamada, *Nat. Commun.*, **5**, 7-17 (2014).
10) D. Maclnnes, M. A. Druy, P. J. Nigrey, D. P. Nairns, A. G. MacDiarmid, A. J. Heeger, *J. Chem. Soc., Chem. Commun.*, **7**, 317 (1981).
11) M. L. Liu, S. J. Visco, L. C. Dejonghe, *J. Electrochem. Soc.*, **138**, 1891 (1991).
12) N. Oyama, T. Tatsuma, T. Sato, T. Sotomura, *Nature*, **373**, 6515, 598 (1995).
13) X. Y. Han, C. X. Chang, L. J. Yuan, T. L. Sun, J. T. Sun, **19**, 12, 1616 (2007).
14) J. Y. Zhang, L. B. Kong, L. Z. Zhan, J. Tang, H. Zhan, Y. H. Zhou, *J. Power Sources*, **168**, 278 (2007).
15) K. Nakahara, S. Iwasa, M. Satoh, Y. Morioka, J. Iriyama, M. Suguro, E. Hasegawa, *Chem. Phys. Lett.*, **359**, 351 (2002).
16) K. Nakahara, J. Iriyama, S. Iwasa, M. Suguro, M. Satoh, E. J. Cairns, *J. Power Sources*, **165**, 398 (2007).
17) M. Armand, S. Grugeon, H. Vezin, S. Laruelle, P. Ribière, P. Poizot, J.-M. Tarascon, *Nature Mater.*, **8**, 120 (2009).
18) Y. Dai, Y. Zhang, L. Gao, G. Xu, J. Xie, A Sodium ion based organic radical battery, *Electrochem. Solid State Lett.*, **13**, 3, A22 (2010).
19) For example, see; (a) L. Zhao, J. Zhao, Y. -S. Hu, H. Li, Z. Zhou, M. Armand, L. Chen, *Adv. Energy Mater.*, **2**, 962 (2012). (b) Y. Park, D. S. Shin, S. H. Woo, N. S. Choi, K. H. Shin, S. M. Oh, K. T. Lee, S. Y. Hong, *Adv. Mater.*, **24**, 3562 (2012)
20) For example, see; (a) S. Wang, L. Wang, Z. Zhu, Z. Hu, Q. Zhao, J. Chen, *Angew. Chem. Int. Ed.*, **53**, 5892 (2014). (b) É. Deunf, N. Dupré, É. Quarez, P.

Soudan, D. Guyomard, F. Dolhem, P. Poizot, *CrystEngComm.*, **18**, 6076 (2016)

21) K. Chihara, N. Chujo, A. Kitajou, S. Okada, *Electrochim. Acta*, **110**, 240 (2013).
22) N. Chujo, K. Chihara, S. Okada, S. Kuze, Japanese patent JP2013-229321A.
23) (a) *Oxocarbons*, ed. R. West, Academic Press, New York, 1980. (b) R. West, J. Niu, in *The Chemistry of the Carbonyl Group*, ed. J. Zabicky, Interscience, London 1970, vol. II, ch.4 (doi:10.1002/ 9780470771228.ch4). (c) F. Sarratosa, *Acc. Chem. Res.*, **16**, 170 (1983). (d) G. Seitz, P. Imming, *Chem. Rev.*, **92**, 1227 (1992).
24) Q. Zhao, J. Wang, Y. Lu, Y. Li, G. Liang, J. Chen, *Angew. Chem. Int. Ed.*, **55**, 12528 (2016).
25) K. Kubota and S. Komaba, *J. Electrochem.* Soc., **162**, A2538, (2015).
26) R. -E. Dinnebier, H. Nuss, M. Jansen, *Acta Cryst.*, **E61**, m2148 (2005).
27) T. Yamashita, H. Momida, T. Oguchi, *Electrochim. Acta*, **195**, 1 (2016).